Cancer Management and Research

Dovepress

open access to scientific and medical research

Open Access Full Text Article

ORIGINAL RESEARCH

RETRACTED ARTICLE: Long Non-Coding RNA *CASC19* Sponges microRNA-532 and Promotes Oncogenicity of Clear Cell Renal Cell Carcinoma by Increasing ETS1 Expression

This article was published in the following Dove Press journal:
Cancer Management and Research

Yu Luo
Feng Liu
Chunhui Yan
Wei Qu
Liang Zhu
Zheng Guo
Fan Zhou
Wei Zhang

Department of Urology, The 161st Hospital of the People's Liberation Army, Wuhan, Hubei 430010, People's Republic of China

Purpose: The long non-coding RNA cancer susceptibility 19 (*CASC19*) is recognized as an important regulator in gastric cancer, colorectal cancer, and non-small cell lung cancer. Nevertheless, to the best of our knowledge, the expression status and detailed roles of *CASC19* in clear cell renal cell carcinoma (ccRCC) have not been elucidated. Hence, we aimed to determine *CASC19* expression in ccRCC and investigate its roles in ccRCC oncogenicity. The molecular mechanisms underlying *CASC19* functions in ccRCC were also determined.

Methods: *CASC19* expression was measured by using reverse transcription-quantitative polymerase chain reaction. The effects of *CASC19* on ccRCC cell proliferation, colony formation, migration, and invasiveness in vitro, as well as on tumor growth in vivo, were examined by the MTT assay, colony formation assay, cell migration and invasiveness assays, and tumor xenograft in nude nice, respectively.

Results: *CASC19* was overexpressed in ccRCC tissues and cell lines. High expression of *CASC19* was closely associated with unfavorable clinicopathological parameters and predicted negative clinical outcomes in patients with ccRCC. Knockdown of *CASC19* decreased ccRCC cell proliferation, colony formation, migration, and invasiveness, as well as attenuated tumor growth in vivo. Mechanistically, *CASC19* functioned as a competing endogenous RNA and upregulated the expression of ETS proto-oncogene 1 (ETS1) through sponging microRNA-532 (miR-532). Furthermore, rescue assays revealed that inhibiting miR-532 or restoring ETS1 expression partially abolished the impacts of *CASC19* knockdown on ccRCC cells.

Conclusion: The CASC19/miR-532/ETS1 regulatory pathway is crucial for the malignant manifestations of ccRCC, which makes it an attractive target for potential treatments of ccRCC.

Keywords: cancer, MTT assay, cell migration, invasiveness, xenograft, knockdown

Introduction

Renal cell carcinoma (RCC) that occurs in the renal cortex ranks as the third leading cause of cancer-associated deaths globally.[1] RCC is characterized by the absence of typical clinical symptoms, diversity of clinical manifestations, and lack of response to radiochemotherapy.[2] It is estimated that there would be approximately 295,000 newly diagnosed RCC cases and 134,000 mortalities due to RCC worldwide.[3] Clear cell RCC (ccRCC), the most common subtype of RCC, accounts for nearly 80% of all diagnosed cases. Until now, multiple factors, such as smoking, excessive drinking, hypertension, and obesity, have been verified to be implicated in

Correspondence: Feng Liu
Department of Urology, The 161st Hospital of the People's Liberation Army, No. 68, Huangpu Road, Wuhan, Hubei 430010, People's Republic of China
Email liufwh@163.com

submit your manuscript | www.dovepress.com
DovePress
http://doi.org/10.2147/CMAR.S242472

ccRCC pathogenesis.[4] Nephrectomy remains the primary therapeutic approach for ccRCC patients diagnosed at an early stage. However, there is still lack of effective treatment for ccRCC patients in the late stage.[5,6] Despite the tremendous development of treatment strategies, the prognosis of ccRCC patients with local or distant metastasis remains unfavorable, with a 5-year survival of less than 10%.[7] Hence, it is critical to understand in detail the mechanisms underlying the occurrence and development of ccRCC, as this knowledge will enable more effective therapeutic strategies.

Non-coding RNAs (ncRNAs) are RNA transcripts that do not code for proteins. According to their length, ncRNAs are classified into two groups: small non-coding RNAs (sncRNAs) and long non-coding RNAs (lncRNAs). LncRNAs are a family of transcripts with a length over 200 nucleotides.[8] Although lncRNAs lack the functional protein coding ability, lately they have been found to exert crucial modulatory effects on cancer initiation and progression.[9] LncRNAs may play oncogenic roles in ccRCC progression when they are overexpressed, or serve as tumor suppressors when their expression level is attenuated.[10]

MicroRNAs (miRNAs) are sncRNAs that are 20–[illegible] nucleotides long.[11] miRNAs effectively regulate gene expression by directly binding to the 3′-untranslated regions (3′-UTRs) of respective complementary messenger RNAs (mRNAs), which promotes degradation and/or suppressed translation of these mRNA.[12] An increasing number of studies report that dysregulation of miRNAs affects various aspects of tumorigenesis and tumor development in almost all human tumor types.[13–15] Specifically, down- and upregulation of various miRNAs, associated a variety of malignant phenotypes, have been documented in ccRCC.[16–19] Therefore, investigating the expression status and biological roles of lncRNAs and miRNAs in ccRCC would facilitate the identification of attractive therapeutic targets for the treatment of patients with this malignancy.

CASC19 has been recognized as an important regulator of gastric cancer,[20] colorectal cancer,[21,22] and non-small cell lung cancer.[23] However, neither the expression pattern nor the functional roles of *CASC19* in ccRCC have been previously defined. In this study, we attempted to detect *CASC19* expression in ccRCC, assess the clinical value of this parameter in patients with ccRCC, and determine the functions of *CASC19* in ccRCC progression. In addition, the molecular mechanisms underlying the oncogenic roles of*CASC19* in ccRCC were elucidated in detail.

Materials and Methods

Patients and Samples

Fifty-one patients diagnosed with ccRCC that underwent nephrectomy in the 161st Hospital of the People's Liberation Army between January 2014 and August 2015 were involved in this study. All samples were collected randomly, and patients that received chemotherapy or radiotherapy before surgical resection were excluded. The obtained ccRCC and adjacent normal renal tissues were immediately frozen in liquid nitrogen and then stored at −80 °C until the analysis. The present study was approved by the Research Ethics Committee of the 161st Hospital of People's Liberation Army. Written informed consent was obtained from all patients enrolled.

Cell Culture

Three ccRCC cell lines, 786-O, Caki-1, and A498, were purchased from the Cell Bank of Type Culture Collection of the Chinese Academy of Sciences (Shanghai, China) and cultured in Dulbecco's modified Eagle medium (DMEM) with 10% fetal bovine serum (FBS), 100 μL/mL penicillin, and 100 mg/mL streptomycin (all from Gibco; Thermo Fisher Scientific Inc., Waltham, MA, USA). The normal human proximal tubule epithelial HK-2 cell line was obtained from the American Type Culture Collection (Manassas, VA, USA) and maintained in Keratinocyte Serum Free Medium (Gibco; Thermo Fisher Scientific, Inc., Waltham, MA, USA). All abovementioned cell lines were grown at 37°C in a humidified atmosphere of 95% air and 5% CO_2.

Reverse Transcription-Quantitative Polymerase Chain Reaction (RT-qPCR)

The extraction of total RNA was conducted by using TRIzol reagent (Invitrogen; Thermo Fisher Scientific, Inc., Waltham, MA, USA) in accordance with the manufacturer's instructions. NanoDrop 2000/2000c (Thermo Fisher Scientific, Inc., Waltham, MA, USA) was utilized to determine total RNA concentration. For miR-532 expression analysis, complementary DNA (cDNA) was prepared from total RNA by using a miScript Reverse Transcription kit (Qiagen GmbH, Hilden, Germany). Next, a miScript SYBR Green PCR kit (Qiagen GmbH, Hilden, Germany) was employed to detect miR-532 expression, with the universal small nuclear RNA U6 as internal control. For the detection of *CASC19* and *ETS1* mRNA levels, reverse transcription was carried out to synthesize cDNA from total RNA by using a PrimeScript RT

reagent kit, followed by qPCR with a SYBR Premix Ex *Taq*™ kit (both from Takara Bio, Dalian, China). The level of *GAPDH* was used as reference for *CASC19* and *ETS1* expression levels. Relative gene expression was analyzed by using the $2^{-\Delta\Delta Cq}$ method.[24]

Subcellular Fractionation Location

The Protein and RNA Isolation System (PARIS) (Life Technologies, CA, USA) was employed to separate the nuclear and cytosolic fractions of ccRCC cells in accordance with the manufacturer's instructions. After RNA isolation, RT-qPCR was performed to evaluate the expression distribution of *CASC19* in ccRCC cells. *GAPDH* and *U6* were used as cytoplasmic and nuclear control transcripts, respectively.

Transfection Experiments

ccRCC cells were inoculated into 6-well plates and incubated at 37°C in the atmosphere of 95% and 5% CO_2 overnight prior to transfection. The miR-532 mimics, miRNA negative control (miR-NC), miR-532 inhibitor, and NC inhibitor were constructed by Guangzhou RiboBio Co., Ltd. (Guangzhou, China).The ETS1 overexpression plasmid pcDNA3.1-ETS1 was synthesized by IBSBio[illegible]S Solutions Co. Ltd, Shanghai, China). Small interfering RNA (siRNA) targeting *CASC19* (si-CASC19) and NC siRNA (si-NC) were obtained from Ge[illegible]pharm Biote[illegible] Co., Ltd. (Shanghai, China). Transfect[illegible] experi[illegible]nts were performed using Lipofectamine 20[illegible]® (In[illegible]gen; Thermo Fisher Scientific, Inc., Waltha[illegible]MA, USA) based on the manufacturer's instructions.

MTT Assay

MTT (3-(4,5-dime[illegible]ylthia[illegible]l-2-yl)-2,5-diphenyltetrazolium bromide) assay was co[illegible]ucted w[illegible] the aim of determining the prolif[illegible]ation o[illegible] ccRCC [illegible]ls. In 24 h following transfection, c[illegible]CC ce[illegible] were inoculated into 96-well plates at a density [illegible] × 10^3 per every well. Cell proliferation was detected at 0, [illegible], 48, and 72 h after seeding by adding 20 μL of 5 mg/mL MTT solution (Sigma-Aldrich; Merck KGaA, Darmstadt, Germany) into each well. The plates were incubated at 37°C in a humidified atmosphere of 95% air and 5% $CO_2$for another 4 h. The culture medium was removed and replaced with 150 μL of dimethyl sulfoxide (Sigma-Aldrich; Merck KGaA, Darmstadt, Germany). Finally, the absorbance at a wavelength of 490 nm was detected by an ELISA microplate reader (Bio-Rad Laboratories, Inc., Hercules, CA, USA).

Colony Formation Assay

Transfected cells were collected and treated as above mentioned. In total, 1 ×103 cells were seeded into each well of the 6-well plates. After 2 week culture, cells were rinsed with phosphate-buffered saline, fixed with 4% paraformaldehyde and stained with 0.1% crystal violet (Sigma-Aldrich; Merck KGaA, Darmstadt, Germany). The formed colonies were imaged and counted under an inverted light microscope (Olympus Corporation, Tokyo, Japan).

Cell Migration and Inva[illegible]ssays

The invasive ability of ccRC[illegible] cells was a[illegible]essed by performing the cell invasiver[illegible]ss a[illegible]y. A total [illegible] 5×10^4 transfected ccRCC cells w[illegible] suspende[illegible] FB[illegible]free DMEM at 48 h post-transfecti[illegible] prior t[illegible]eing ino[illegible]ated into the upper compartments [illegible] tra[illegible]ll cham[illegible]r inserts coated with Matrigel (b[illegible] from BD [illegible]iosci[illegible]nces, Franklin Lakes, NJ, USA). [illegible]MEM containing [illegible]% FBS was added into the lower compartmen[illegible] to serve as the source of chemo attractants. The chambers [illegible]ere then incubated at 37°C in the [illegible]tmosphere [illegible]95% air and 5% CO_2 for 24 h, and the invad[illegible]g cells we[illegible] then fixed with 4% paraformaldehyde and sta[illegible]d wit[illegible]0.1% crystal violet. Five visual fields of each [illegible]hamber insert were randomly chosen, and the average number [illegible] cells was counted under an inverted light microscope. The migratory ability of ccRCC cells was determined by using the same experimental steps as for the cell invasiveness assay, except that the inserts were not coated with Matrigel.

Tumor Xenograft in Nude Nice

The short hairpin RNAs (shRNAs) targeting *CASC19* (sh-CASC19) and NC shRNA (sh-NC; both from Genepharma Biotech Co., Ltd.) were incorporated into a pLKO vector to produce pLKO-sh-CASC19 and pLKO-sh-NC plasmids. The lentiviral constructs were cloned and purchased from Genepharma Biotech Co., Ltd.

Nude mice (4–5 weeks old; 18–20 g) were bought from the Shanghai Laboratory Animal Center (Shanghai, China) and maintained in the specific-pathogen-free environment. All experimental steps in animals and animal care protocols were approved by the Animal Ethics Committee of the 161st Hospital of People's Liberation Army, and were performed under supervise of the Animal Protection Law of the People's Republic of China-2009.A498 cells stably transfected with sh-CASC19 or sh-NC were collected and dispersed in phosphate buffer solution. A total of 1 × 10^7 cells resuspended in phosphate buffer solution were

subcutaneously injected into the flank of nude mice. Each group contained three mice. The width and length of the formed xenograft were measured weekly by using a Vernier caliper. The volume of each tumor xenograft was calculated using the following equation: length × width^2 × 1/2. All nude mice were euthanized at 4 weeks post-inoculation and the tumor xenografts were dissected out and weighed.

Bioinformatics Prediction and Luciferase Reporter Assay

StarBase 3.0 (http://starbase.sysu.edu.cn/) was utilized for the analysis of the lncRNA-miRNA interaction. The fragments of *CASC19* containing the wild-type (wt) complementary or mutated (mut) miR-532 sequences were amplified by Genepharma Biotech Co., Ltd. and subcloned into the pmirGLO plasmid (Promega Corporation, Madison, WI, USA). These chemically synthesized reporter plasmids were defined as CASC19-wt and CASC19-mut, respectively. ccRCC cells were inoculated into 24-well plates one day before transfection. Cells were co-transfected with miR-532 mimics or miR-NC, and CASC19-wt or CASC19-mut, by using Lipofectamine 2000®.Following incubation for 48 hat 37°C, the luciferase activity was determined by using a Dual-Luciferase Reporter Assay system (Promega Corporation, Madison, WI, USA). Renilla luciferase activity was used for normalization of the data.

RNA Immunoprecipitation (RIP) Assay

RIP assay was carried out by using a Magna RIP RNA-binding immunoprecipitation kit (EMD Millipore, New Jersey, USA). Cells were lysed by using RIP lysis buffer supplemented with an RNase inhibitor and protease inhibitor cocktail. Then, the cell lysates were incubated with magnetic beads conjugated with an anti-AGO2 antibody or control IgG (EMD Millipore). Following overnight incubation at 4°C, the magnetic beads were collected and treated with proteinase K. The immunoprecipitated RNA was isolated and quantified by RT-qPCR.

Western Blot Analysis

Total protein was isolated using RIPA assay lysis buffer (Beyotime Institute of Biotechnology, Shanghai, China). Protein concentration was evaluated by a BCA protein assay kit (Beyotime Institute of Biotechnology, Shanghai, China). Equal amounts of protein were separated on 10% SDS-PAGE gels and electrophoretically transferred onto polyvinylidene fluoride membranes (Beyotime Institute of Biotechnology, Shanghai, China). Subsequently, the membranes were blocked with 5% skimmed milk diluted in Tris-buffered saline containing 0.1% Tween-20 (TBST) and incubated overnight at 4 °C with the following primary antibodies (Abcam, Cambridge, UK): rabbit anti-human ETS1 antibody (1:1000 dilution; cat. no. ab220361) and rabbit anti-human GAPDH antibody (1:1000 dilution; cat. no. ab181603). After rinsing with TBST, a horseradish peroxidase-conjugated secondary antibody (1:5000 dilution; cat. no. ab6721; Abcam) was added, and the membranes were incubated at room temperature for an additional 2 h. The protein signals were visualized by using an electrochemiluminescence advanced Western blot detection kit (Thermo Fisher Scientific, Waltham, MA, USA). GAPDH signal was used for data normalization.

Statistical Analysis

Data are presented as the mean ± standard error of the mean. All statistical analyses were performed by using SPSS 20.0 (IBM Corp., Armonk, NY, USA). The chi-squared test was applied for assessing the correlation between *CASC19* expression and clinicopathological parameters in ccRCC patients. The differences between two groups were analyzed by the Student's *t*-test. The one-way analysis of variance followed, if appropriate, by the Student-Newman-Keuls post hoc test for multiple comparisons was utilized for the comparison of the differences between more than two groups. The overall survival curves were plotted using the Kaplan-Meier method and analyzed by the Log rank test. The Spearman correlation analysis was used to examine the association between *CASC19* and miR-532 levels in ccRCC tissues. All statistical analyses were conducted with a significance level of $P< 0.05$.

Results

High *CASC19* Expression Predicts Poor Prognosis in ccRCC

To investigate the clinical relevance of *CASC19* expression in ccRCC, RT-qPCR was carried out to measure *CASC19* level in 51 pairs of ccRCC and adjacent normal renal tissue samples. *CASC19* expression level was higher in ccRCC tissues than in adjacent normal renal tissues (Figure 1A). Relative *CASC19* expression was also determined in ccRCC cell lines, and *CASC19* was found to be upregulated in all three ccRCC cell lines when compared

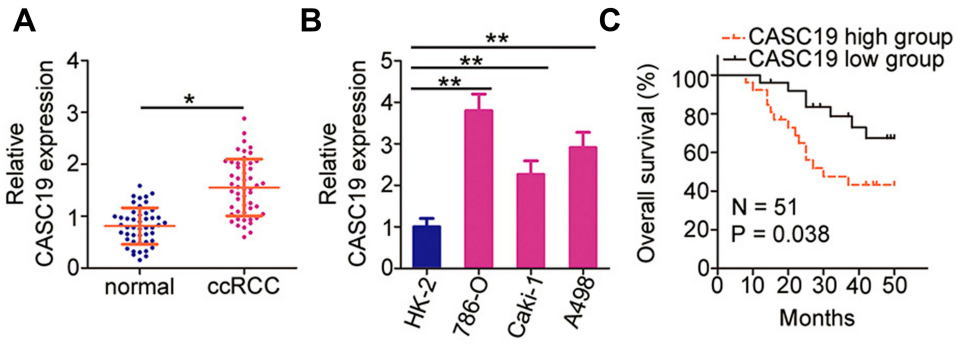

Figure 1 Upregulation of *CASC19* in ccRCC tissues and cell lines (**A**) Relative *CASC19* expression detected in 51 pairs of ccRCC and adjacent normal renal tissue samples by using RT-qPCR.(**B**) *CASC19* expression levels determined by RT-qPCR in three ccRCC cell lines (786-O, Caki-1, and A498) and the normal human proximal tubule epithelial cell line HK-2. (**C**) ccRCC patients with high *CASC19* expression had much lower overall survival rate than those with low *CASC19* expression (P = 0.038). Statistical significance of differences is indicated as follows: **P* <0.05 and ***P* <0.01.

with its expression level in the normal human proximal tubule epithelial HK-2 cell line (Figure 1B).

To analyze the relationship between *CASC19* and clinical parameters in ccRCC, all 51 patients were separated into either *CASC19* high or *CASC19* low expression groups. The median value of *CASC19* expression level in the ccRCC tissue was defined as the cutoff value. Correlation analyses demonstrated that ccRCC patients with high *CASC19* expression tended to have larger tumor sizes ($P = 0.045$), more advanced TNM stage (P = 0.012), and more frequently have lymph node metastasis ($P = 0.003$) (Table 1). In addition, patients with ccRCC having high *CASC19* expression exhibited much lower overall survival rate than those with low *CASC19* expression (Figure 1C, P = 0.038). These results implied that *CASC19* may perform an important part in the progression of ccRCC.

Knockdown of *CASC19* Attenuates ccRCC Cell Proliferation, Colony Formation, Migration, and Invasiveness in vitro

Among the three ccRCC cell lines tested, 786-O and A498 cell lines had relatively higher *CASC19* expression, so these two cell lines were chosen for the functional assays. As *CASC19* was upregulated in both ccRCC tissues and cell lines, we hypothesized that *CASC19* might play a tumor-promoting role in ccRCC progression. To verify this hypothesis, 786-O and A498 cells were transfected with si-CASC19 to silence endogenous *CASC19* expression. After transfection, RT-qPCR analysis demonstrated that *CASC19* was significantly knocked down in si-CASC19-transfected 786-O and A498 cells relative to its level in cells transfected with si-NC (Figure 2A). By using the MTT and colony formation assays, we observed that *CASC19* knockdown impaired the proliferative (Figure 2B) and colony-forming abilities (Figure 2C) of 786-O and A498 cells. Furthermore, the migration (Figure 2D) and invasiveness (Figure 2E) of 786-O and A498 cells was markedly attenuated by *CASC19* silencing, as suggested by the results of the cell migration and invasion assays. Thus, *CASC19* might indeed play a prominent role in ccRCC oncogenicity.

Table 1 The Correlation Between the Expression of *CASC19* and Clinicopathological Parameters of Patients with ccRCC

Clinicopathological Parameters	CASC19 Expression		P value
	High	Low	
Gender			0.779
Male	16	14	
Female	10	11	
Age			0.404
<60 years	12	15	
≥ 60 years	14	10	
Tumor size			0.045
<4 cm	11	18	
≥ 4 cm	15	7	
Grade			0.089
Grade 1+2	7	13	
Grade 3+4	19	12	
TNM stage			0.012
I+II	9	18	
III+IV	17	7	
Lymph node metastasis			0.003
Negative	11	21	
Positive	15	4	

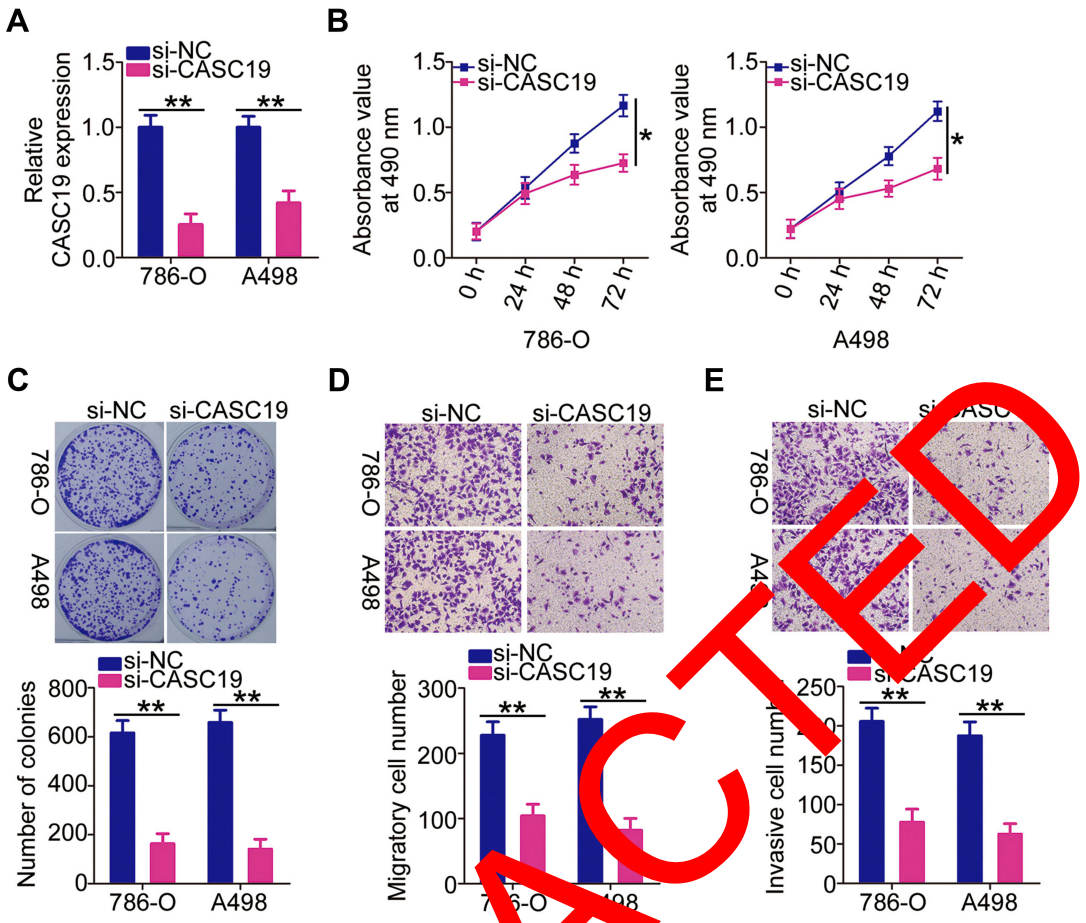

Figure 2 Attenuation of 786-O and A498 cell proliferation, migrati[on] [in]vasiveness in vitro by *CASC19* knockdown (**A**) *CASC19* levels determined by RT-qPCR in 786-O and A498 cells transfected with si-CASC19 or si-NC. (**B, C**) T[he] modula[tory] effect[s] of *CASC19* downregulation on the proliferation and colony formation of 786-O and A498 cells determined by the MTT and colony formation a[ssa]ys. (**D, E**) [Mi]gratory ar[d] invasive capacities of 786-O and A498 cells measured by the cell migration and invasion assays after *CASC19* knockdown. Statistical significa[nce] of diffe[rences] [in]dicated as follows: *P<0.05 and **P <0.01.

CASC19 Functions as a Competing Endogenous RNA (ceRNA) for miR-532 and Consequently Positively Modulates ETS1 Expression in ccRCC Cells

It has been shown previously that lncRNAs may function as ceRNAs to interact with miRNAs in the cytoplasm, thereby reducing the suppressive action of miRNAs on their targets. In order to investigate whether *CASC19* acts as a ceRNA, we first determined the expression distribution of *CASC19* in 786-O and A498 cells. Subcellular fractionation location plus RT-qPCR analysis indicated that *CASC19* was mainly distributed in the cytoplasm of 786-O and A498 cells (Figure 3A).Next, bioinformatics analysis was employed to search for the miRNAs that might potentially interact with *CASC19*. As shown in Figure 3B, miR-532 was predicted to contain a putative binding site for *CASC19*.Thus, miR-532 was selected for further verification because this miRNA was revealed to be downregulated in ccRCC and participate in cancer progression.[26]

After confirming the efficiency of miR-532 mimics (Figure 3C), we performed the luciferase reporter assay to determine the interaction between miR-532 and *CASC19* in ccRCC cells. We found that the luciferase activity was strongly reduced in 786-O and A498 cells co-transfected with miR-532 mimics and *CASC19*-wt (Figure 3D). In contrast, co-transfection with miR-532 mimics and *CASC19*-mut failed to affect luciferase activity. The RIP assay was applied to further evaluate whether miR-532 and *CASC19* co-localize in the same RNA-induced silencing complex. We found that miR-532 and *CASC19* were enriched in the AGO2-immunoprecipitated complex relative to that in the IgG-immunoprecipitated one (Figure 3E). Furthermore, miR-532 was significantly downregulated in ccRCC tissues compared with its level in adjacent normal renal tissues (Figure 3F). A correlation analysis indicated that *CASC19*

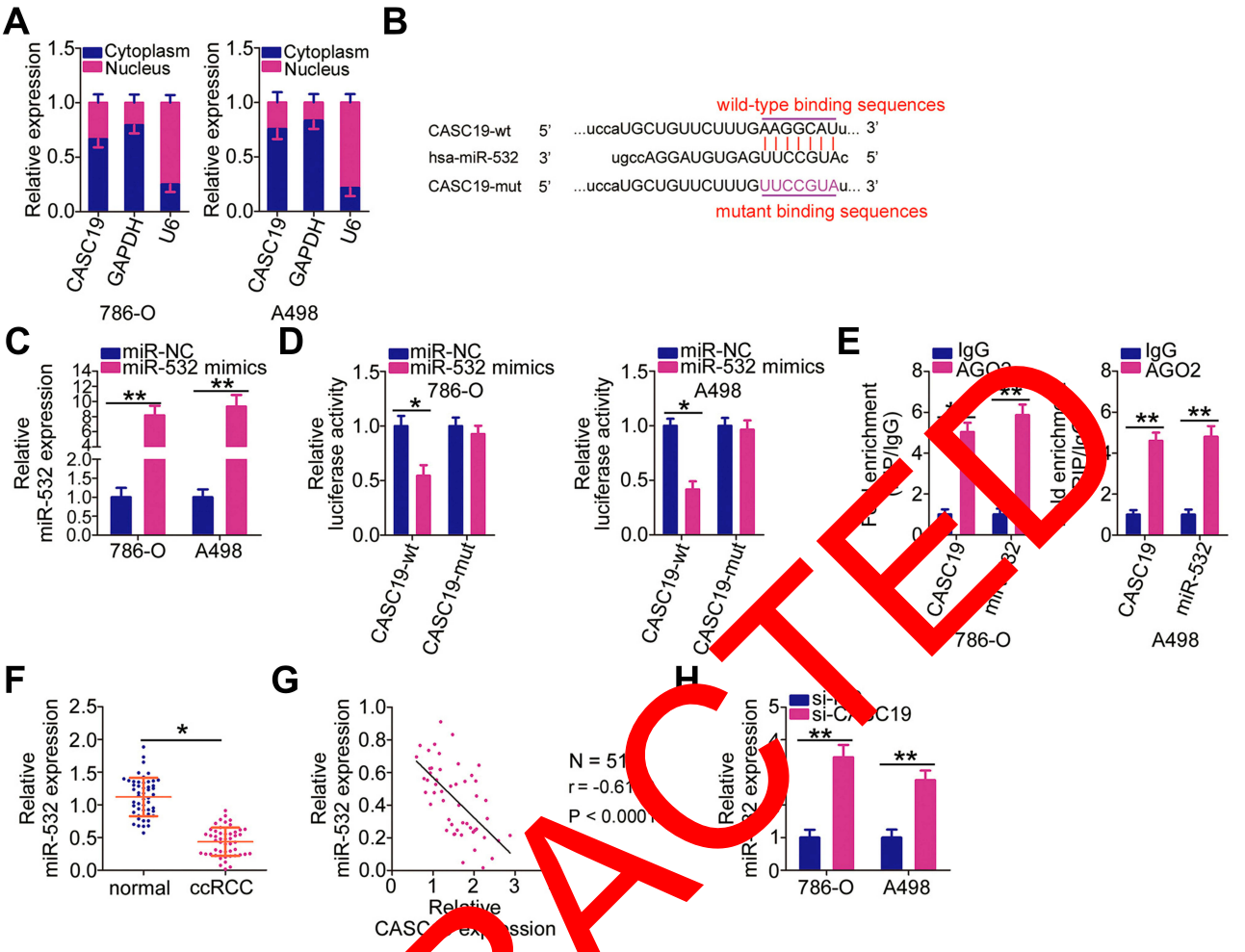

Figure 3 *CASC19* functions as a molecular sponge for miR-532 in cells. (**A**) 786-O and A498 cells were fractionated into nuclear and cytosolic fractions. Total RNA of each fraction was isolated and *CASC19* expression levels determined by using RT-qPCR. (**B**) The schematic of miR-532 wild-type (wt) and mutant (mut) targeting sites within *CASC19*. (**C**) miR-532 levels in 786-O and A498 cells transfected with miR-532 mimics or miR-NC were measured by RT-qPCR. (**D**) Luciferase activity of the *CASC19*-wt or *CASC19*-mut constructs determined in the presence of miR-532 mimics or miR-NC. (**E**) 786-O and A498 cell lysates were immunoprecipitated with AGO2 or IgG antibodies. The immunoprecipitated RNA was subjected to RT-qPCR analysis to quantify miR-532 and *CASC19* levels. (**F**) miR-532 expression levels in 51 pairs of ccRCC and adjacent normal renal tissue samples determined by using RT-qPCR. (**G**) Correlation between miR-532 and *CASC19* expression levels in 51 ccRCC tissue samples (r = −0.6180, $P < 0.0001$). (**H**) miR-532 expression levels in *CASC19*-deficient 786-O and A498 cells determined by using RT-qPCR. Statistical significance of differences is indicated as follows: *$P < 0.05$ and **$P < 0.01$.

expression level was inversely correlated with that of miR-532 in the 51 samples of ccRCC tissues (Figure 3G; r = −0.6180, $P < 0.0001$). Besides, RT-qPCR analysis uncovered the inverse relationship between miR-532 and *CASC19* expression levels in 786-O and A498 cells (Figure 3H).

ETS1 has been identified as a direct target of miR-532 in ccRCC.[26] Therefore, we subsequently attempted to clarify the effect of *CASC19* on ETS1 expression. RT-qPCR and Western blotting were performed to detect ETS1 mRNA and protein expression in 786-O and A498 cells after transfection with si-CASC19 or si-NC. The expression levels of ETS1 mRNA (Figure 4A) and protein (Figure 4B) after si-CASC19 treatment were significantly lower than those in si-NC-transfected 786-O and A498 cells. Furthermore, *ETS1* mRNA expression was significantly higher in ccRCC tissues than in adjacent normal renal tissues (Figure 4C). A positive correlation between expression levels of *CASC19* and *ETS1* mRNAs were identified in ccRCC tissue samples (Figure 4D; r = 0.4738, $P = 0.0004$). The correlation between *ETS1* mRNA and miR-532 in ccRCC tissues was also analyzed. Spearman correlation analysis displayed that *ETS1* mRNA was inversely correlated with miR-532 in ccRCC tissues (Figure 4E; r = −0.5296, $P = 0.0010$). To elucidate whether *CASC19* controls *ETS1* expression via sponging miR-532, the rescue assays were conducted in *CASC19*-deficient786-O and A498 cells after further transfection with the miR-532 inhibitor or NC inhibitor. RT-qPCR verified the successful silencing of miR-532 expression in 786-O and A498 cells

that were transfected with the miR-532 inhibitor (Figure 4F). ETS1 mRNA (Figure 4G) and protein (Figure 4H) levels, which were decreased by *CASC19* knockdown, were almost fully recovered in 786-O and A498 cells after their co-transfection with the miR-532 inhibitor. Taken together, these results suggested that *CASC19* competitively sponged miR-532 and thereby positively modulated ETS1 expression.

CASC19 Exerts Its Cancer-Promoting Roles in ccRCC Cells via Modulating the miR-532/ETS1 Axis

To investigate whether the oncogenic actions of *CASC19* in ccRCC cells were mediated through the regulation of the miR-532/ETS1 axis, a series of rescue assays were performed in 786-O and A498 cells. First, a combination of si-GASC19, plus miR-532 inhibitor or NC inhibitor was co-transfected into 786-O and A498 cells, and changes in the proliferation, migration, and invasiveness were evaluated. Inhibition of miR-532 expression abrogated the inhibitory effects of *CASC19* knockdown on the proliferation (Figure 5A), colony formation (Figure 5B), migration (Figure 5C), and invasiveness (Figure 5D) of 786-O and A498 cells. Next, *ETS1* overexpression plasmid pcDNA3.1-ETS1 or empty pcDNA3.1 plasmid in combination with si-CASC19 was co-transfected into 786-O and A498 cells. Western blot analysis confirmed that transfection with pcDNA3.1-ETS1 resulted in a significant upregulation of ETS1 in 786-O and A498 cells (Figure 6A). Functional experiments showed that the impacts of *CASC19* knockdown on the proliferation (Figure 6B), colony formation (Figure 6C), migration (Figure 6D), and invasiveness (Figure 6E) of 786-O and A498 cell[illegible] eliminated by means of pcDNA3.1-ETS1 restora[illegible]n. These r[illegible]lts clearly demonstrated that the miR-532/ETS[illegible]xis was resp[illegible]nsible for the oncogenic roles of *CAS[illegible]9* in ccRC[illegible] cells.

Interference [illegible] *CA[illegible]19* Su[illegible]presses Tumor Gr[illegible]th of cc[illegible] Cells in vivo

A tumor xenograft [illegible]odel was constructed by subcutaneous[illegible]jecting A49[illegible]ells stably transfected with sh-CA[illegible]19 or sh-NC into the flank of nude mice. The

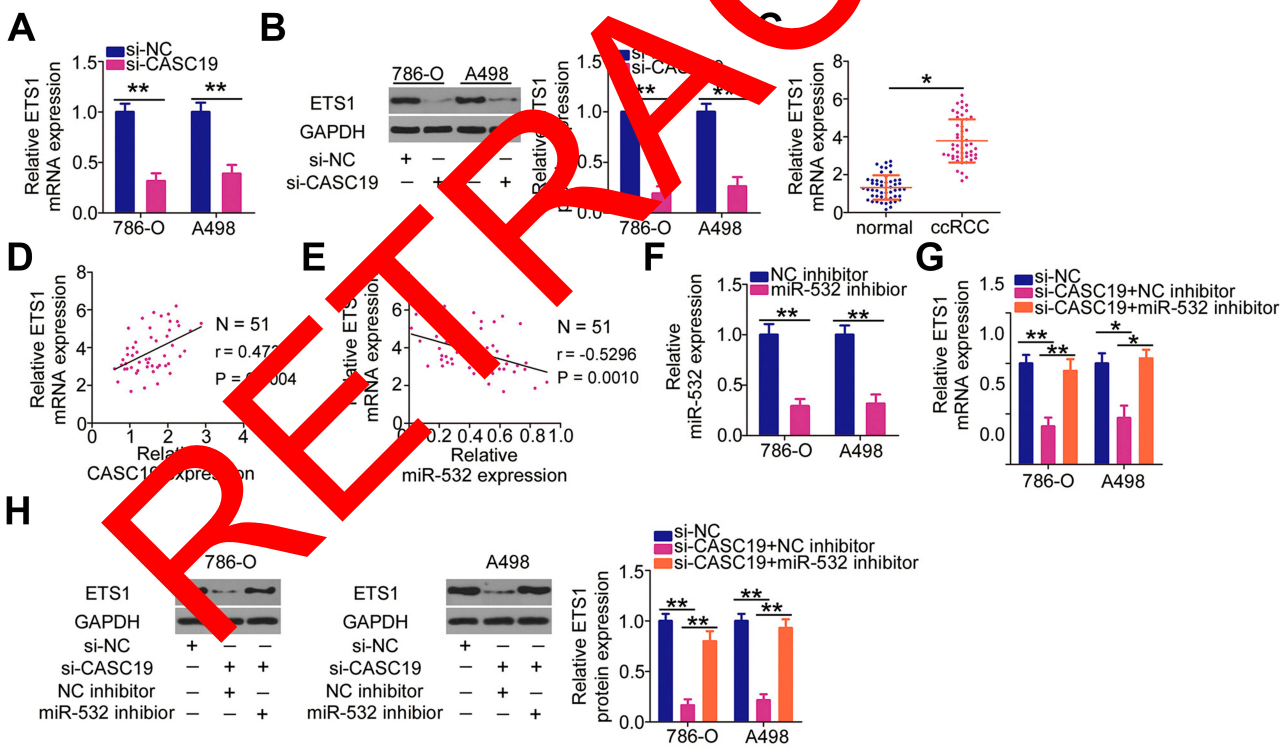

Figure 4 *CASC19* directly sponges miR-532 expression and thereby positively regulates *ETS1* expression in ccRCC tissues. (**A, B**) Effects of *CASC19* silencing on ETS1 mRNA and protein expression levels in 786-O and A498 cells determined by using RT-qPCR and Western blotting, respectively. (**C**) Expression of *ETS1* mRNA in ccRCC and adjacent normal renal tissues analyzed by using RT-qPCR. (**D**) Correlation between expression levels of *CASC19* and *ETS1* mRNA in 51 samples of ccRCC tissues (r = 0.4738, *P* = 0.0004). (**E**) Correlation between expression levels of miR-532 and *ETS1* mRNA in 51 samples of ccRCC tissues (r = −0.5296, *P* = 0.0010). (**F**) miR-532 expression levels in 786-O and A498 cells at 48 h after transfection with the miR-532 inhibitor or NC inhibitor. (**G, H**) ETS1 mRNA and protein expression levels quantified by RT-qPCR and Western blotting, respectively, in 786-O and A498 cells transfected with si-CASC19 and either the miR-532 inhibitor or NC inhibitor. Statistical significance of differences is indicated as follows: **P* <0.05 and ***P* <0.01.

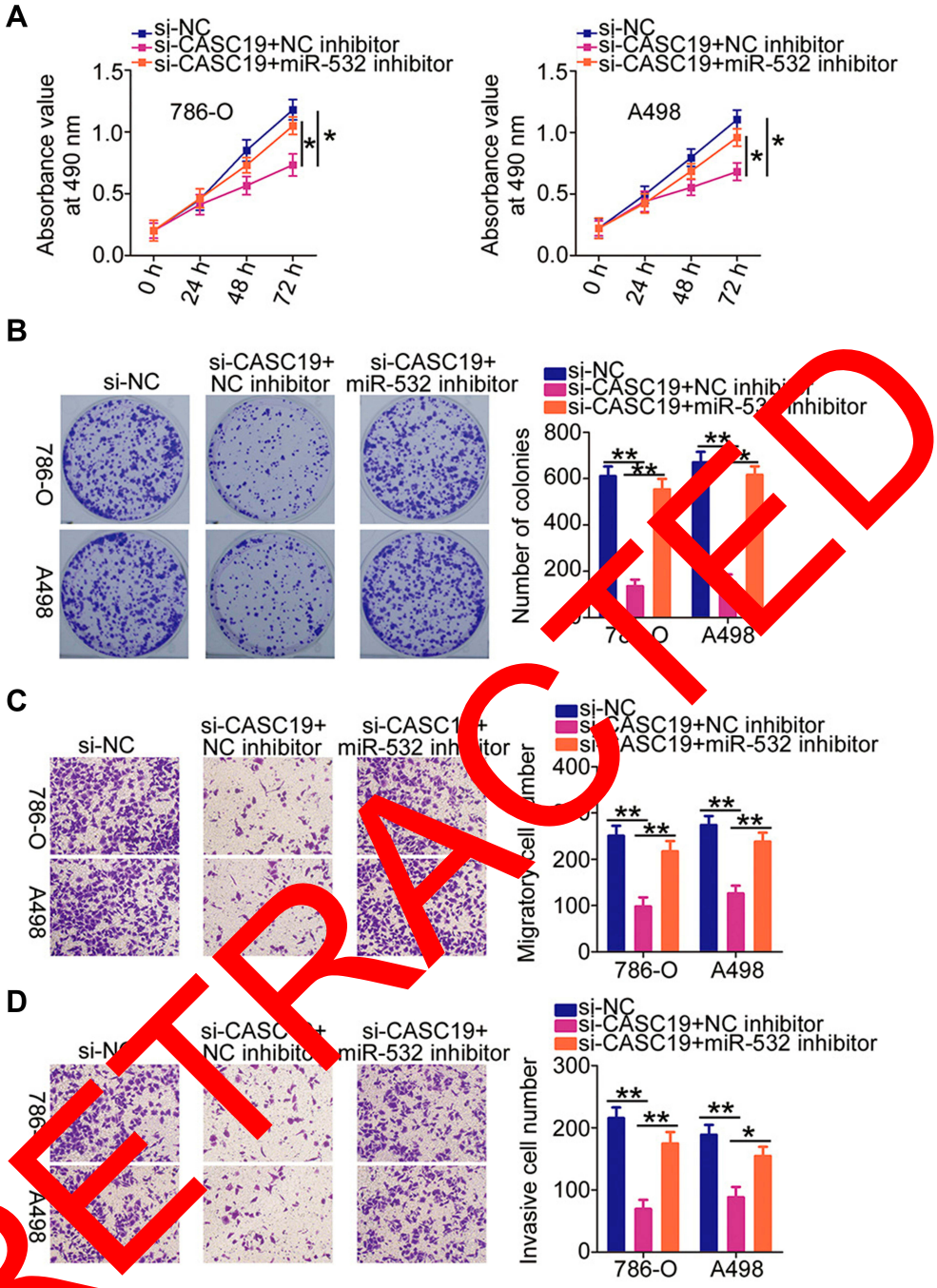

Figure 5 Inhibition of miR-532 alleviates the inhibitory effects of *CASC19* knockdown in 786-O and A498 cells. (**A**–**D**) Proliferation, colony formation, migration, and invasiveness properties of 786-O and A498 cells after co-transfection with si-CASC19 and either miR-532 inhibitor or NC inhibitor determined in the MTT, colony formation, cell migration and invasion assays. *P <0.05 and **P <0.01.

decrease in *CASC19* expression was confirmed in A498 cells stably transfected with sh-CASC19, as quantified by RT-qPCR (Figure 7A). The volume (Figure 7B) and size (Figure 7C) of tumor xenografts was strongly decreased in the sh-CASC19 group compared with these parameters in the sh-NC group. The weight of tumor xenografts was measured when the nude mice were euthanized 4 weeks post-inoculation. The reduction of tumor weight was observed in the nude mice that were inoculated with sh-CASC19 stably-transfected A498 cells (Figure 7D). In addition, expression of miR-532 was upregulated (Figure 7E) in the sh-CASC19 group. Furthermore, Western blotting indicated that ETS1 protein amount was decreased in the sh-CASC19 tumor xenografts

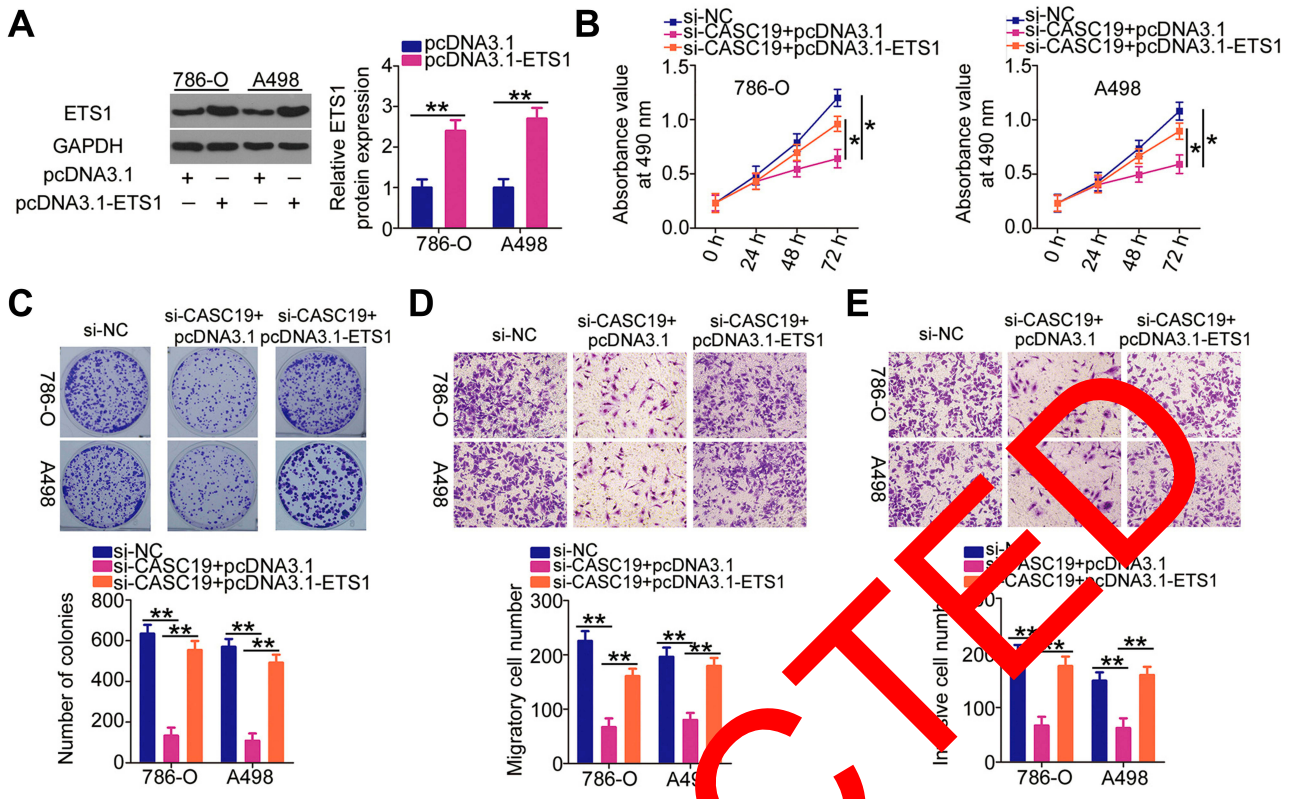

Figure 6 Restoration of *ETS1* expression abrogates the inhibitory effects of *CASC19* knockdown on 786-O and A498 cells. (**A**) ETS1 protein expression in 786-O and A498 cells transfected with pcDNA3.1-ETS1 or pcDNA3.1 measured by Western blot. (**B**–**E**) Proliferation, colony formation, migration, and invasiveness properties of 786-O and A498 cells after their co-transfection with si-CASC19 and either pcDNA3.1-ETS1 or pcDNA3.1 determined in the MTT, colony formation, cell migration and invasion assays. Statistical significance of differences is indicated as follows: **P* <0.05 and ***P* <0.01.

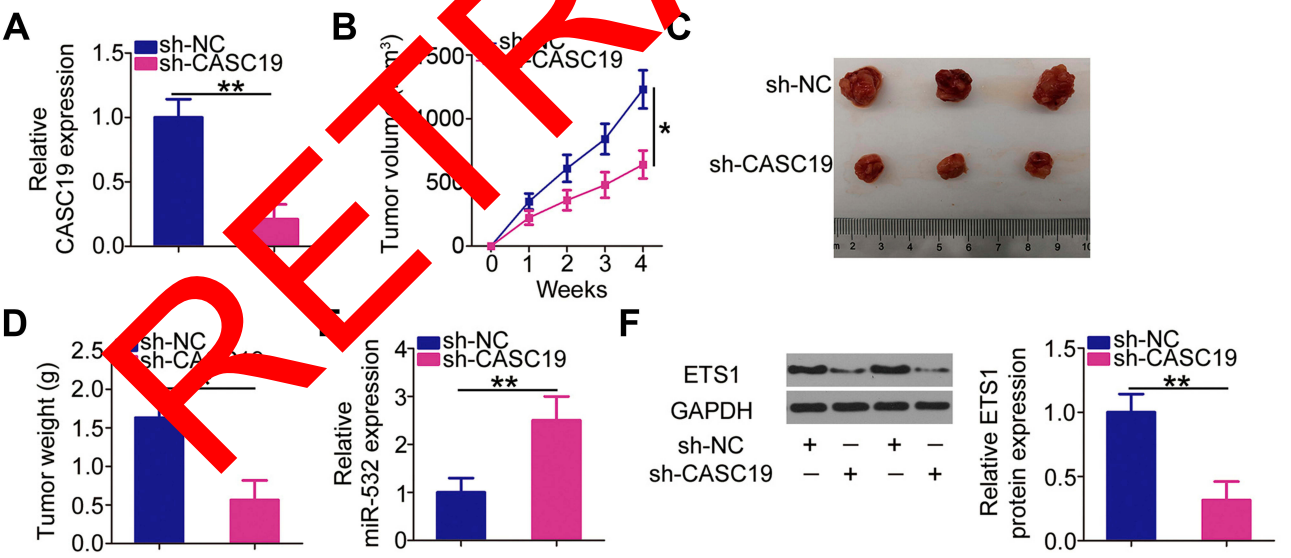

Figure 7 *CASC19* depletion impairs tumor growth of ccRCC cells in vivo. (**A**) *CASC19* expression in A498 cells stably transfected with sh-CASC19 quantified by using RT-qPCR. (**B**) Weekly measurements of tumor xenograft volume. (**C**) Representative images of tumor xenografts obtained from ccRCC cells transfected with sh-CASC19 and sh-NC. (**D**) Tumor xenograft weight determined when the nude mice were euthanized at 4 weeks post-inoculation. (**E**) miR-532 expression level in tumor xenografts quantified by using RT-qPCR. (**F**) Western blot analysis of ETS1 protein expression in tumor xenografts. Statistical significance of differences is indicated as follows: **P* <0.05 and ***P* <0.01.

(Figure 7F). Collectively, silenced *CASC19* expression impaired tumor growth of ccRCC cells in vivo.

Discussion

Dysregulation of lncRNAs in ccRCC has been documented in many studies.[27,28] LncRNAs may exert pro-oncogenic or anti-oncogenic effects, and they play an important role in promoting or preventing ccRCC progression.[29–31] Therefore, detailed elucidation of lncRNA roles and mechanisms underlying dysregulation of lncRNAs in ccRCC may be instrumental for the development of promising novel therapeutic approaches for patients with this disease. Although expression profiles of some lncRNAs associated with ccRCC have been described previously, there are still numerous lncRNAs with unclear expression pattern, whose roles in ccRCC have not been clarified. In this study, we determined *CASC19* expression in ccRCC and investigated the clinical importance of this lncRNA in patients with ccRCC. In addition, we examined biological actions of *CASC19* on the aggressive features of ccRCC tumors and explored the mechanisms underlying these effects.

CASC19 is a well-studied lncRNA in several human cancer types. For example, *CASC19* expression is increased in advanced gastric cancer and apparently associated with the higher pathologic TNM stage, pathologic T stage, lymph node metastasis, and poor overall survival.[20] In addition, multivariable Cox analysis identified *CASC19* as an independent prognostic factor for predicting the overall survival of patients with gastric cancer.[20] *CASC19* is also highly expressed in colorectal[21,22] and non-small cell lung cancers.[23] However, the expression pattern of *CASC19* in ccRCC has not been thoroughly investigated. In this study, our results showed that *CASC19* was upregulated in ccRCC tissues and cell lines. The high *CASC19* expression significantly correlated with tumor size, advanced TNM stage and lymph node metastasis in patients with ccRCC. Notably, ccRCC patients with high *CASC19* expression had shorter overall survival than patients with low CASC19 expression.

CASC19 has been demonstrated to have pro-oncogenic actions during carcinogenesis and cancer progression. For example, interference with *CASC19* expression restricted colorectal cancer cell proliferation, migration, invasiveness and epithelial-mesenchymal transition in vitro.[21,22] In non-small cell lung cancer, a reduction of *CASC19* expression suppressed cell growth and metastasis in vitro.[23] Nevertheless, to the best of our knowledge, the roles of *CASC19* in ccRCC have not been elucidated in detail. Herein, data from functional experiments confirmed the oncogenic actions of *CASC19* and demonstrated that *CASC19* promoted ccRCC cell proliferation, colony formation, migration, and invasiveness in vitro, as well as tumor growth in vivo.

It is well established that lncRNAs located in the cytoplasm affect a wide range of physiological processes by acting as ceRNAs.[32] LncRNAs competitively bind to miRNAs and consequently alleviate the impact of miRNAs on their targets. As a result, the expression level of mRNAs targeted by miRNAs increases.[25] Hence, we subsequently explored the highly complex mechanisms underlying the tumor-promoting activities of *CASC19* in ccRCC cells. Firstly, subcellular fractionation location plus RT-qPCR analysis revealed that *CASC19* was mainly distributed in the cytoplasm of ccRCC cells, suggesting that *CASC19* could work as a ceRNA. Second, bioinformatics analysis predicted that miR-532 contains a putative binding site for *CASC19*. Third, the direct binding and interaction between *CASC19* and miR-532 in ccRCC cells was verified by the luciferase reporter and RIP assays, respectively. Fourth, expression of miR-532 was negatively regulated by *CASC19* both in vitro and in vivo. Fifth, *CASC19* positively modulated the expression of *ETS1* in ccRCC cells, and the positive regulation effects were abrogated through sponging miR-532. These results provide sufficient evidence to demonstrate that *CASC19* functions as a miR-532 sponge and increases the expression of *ETS1* in ccRCC cells.

miR-532 attenuates ccRCC oncogenicity, but its level is downregulated in ccRCC.[26] Mechanistic studies validated *ETS1* as a gene directly targeted by miR-532 in ccRCC.[26] ETS1 protein is a member of the ETS family of transcription factors that directly interact with specific DNA sequences containing a GGAA/T core motif.[33] ETS1 is overexpressed in a number of human cancers, such as breast cancer,[34] cervical cancer,[35] and gastric cancer.[36] ETS1 is upregulated in ccRCC[37] and has a promoting effect on the malignancy of this cancer.[18] In this study, we found that *ETS1* expression was positively modulated by *CASC19* in ccRCC. Furthermore, our results revealed that the miR-532/ETS1 axis is essential for the tumorigenic activities of *CASC19* in ccRCC. Apparently, the CASC19/miR-532/ETS1 regulatory pathway is crucial for the malignant manifestations of ccRCC, which makes it an attractive target for future drug discovery projects.

The use of siRNA in the tumor xenograft in nude nice assay was a limitation in the present study. In our future experiments, short hairpin RNA against *CASC19* will be used to verify the in vivo results.

Conclusion

In summary, *CASC19* is overexpressed in ccRCC and high level of its expression was associated with worse clinical outcomes. *CASC19* functions as an oncogenic lncRNA that promotes the occurrence and development of ccRCC by acting as a ceRNA for miR-532 and thereby promoting *ETS1* expression. Our findings substantially improve our knowledge about the roles of *CASC19*, miR-532, and *ETS1* in ccRCC, as well as help to identify promising novel therapeutic targets for ccRCC.

Ethics and Consent Statement

The present study was approved by the Ethics Committee of The 161st Hospital of the People's Liberation Army and performed in accordance with the Declaration of Helsinki and the guidelines of the Ethics Committee of The 161st Hospital of People's Liberation Army. Written informed consent was obtained from all patients for the use of their clinical tissues. All experimental steps in animals and animal care protocols were approved by the Animal Ethics Committee of the 161st Hospital of People's Liberation Army, and were performed under supervise of the Animal Protection Law of the People's Republic of China-2009.

Data Sharing Statement

The datasets used and/or analyzed during the present study are available from the corresponding author on reasonable request.

Funding

This study has not received any specific funding.

Disclosure

The authors declare that they have no competing interests in this work.

References

1. Garcia JA, Cowey CL, Godley PA. Renal cell carcinoma. *Curr Opin Oncol*. 2009;21(3):266–271. doi:10.1097/CCO.0b013e32832a05c8
2. Sourbier C, Danilin S, Lindner V, et al. Targeting the nuclear factor-kappaB rescue pathway has promising future in human renal cell carcinoma therapy. *Cancer Res*. 2007;67(24):11668–11676. doi:10.1158/0008-5472.CAN-07-0632
3. Hsieh JJ, Purdue MP, Signoretti S, et al. Renal cell carcinoma. *Nature Rev Dis Primers*. 2017;3:17009. doi:10.1038/nrdp.2017.9
4. Chow WH, Dong LM, Devesa SS. Epidemiology and risk factors for kidney cancer. *Nature Rev Urol*. 2010;7(5):245–257. doi:10.1038/nrurol.2010.46
5. Greef B, Eisen T. Medical treatment of renal cancer: new horizons. *Br J Cancer*. 2016;115(5):505–516. doi:10.1038/bjc.2016.230
6. Ljungberg B, Bensalah K, Canfield S, et al. EAU guidelines on renal cell carcinoma: 2014 update. *Eur Urol*. 2015;67(5):913–924. doi:10.1016/j.eururo.2015.01.005
7. Cohen HT, McGovern FJ. Renal-cell carcinoma. *N Engl J Med*. 2005;353(23):2477–2490. doi:10.1056/NEJMra043172
8. Ponting CP, Oliver PL, Reik W. Evolution and functions of long noncoding RNAs. *Cell*. 2009;136(4):629–641. doi:10.1016/j.cell.2009.02.006
9. Schmitt AM, Chang HY. Long noncoding RNAs in cancer pathways. *Cancer Cell*. 2016;29(4):452–463. doi:10.1016/j.ccell.2016.03.010
10. Liu X, Hao Y, Yu W, et al. Long non-coding RNA emergence during renal cell carcinoma tumorigenesis. *Cell Physiol Biochem*. 2018;47(2):735–746. doi:10.1159/000490026
11. Filipowicz W, Bhattacharyya SN, Sonenberg N. Mechanisms of post-transcriptional regulation by microRNAs: are the answers in sight? *Nature Rev Genet*. 2008;9(2):102–114. doi:10.1038/nrg2290
12. Grange C, Collino F, Tapparo M, Camussi G. Oncogenic micro-RNAs and renal cell carcinoma. *Front Oncol*. 2014;4:49. doi:10.3389/fonc.2014.00049
13. Garzon R, Calin GA, Croce CM. MicroRNAs in cancer. *Annu Rev Med*. 2009;60:167–179. doi:10.1146/annurev.med.59.053006.104707
14. Garzon R, Croce CM. MicroRNAs and cancer production. *Semin Oncol*. 2011;38(6):721–726. doi:10.1053/j.seminoncol.2011.08.008
15. Garzon R, Marcucci G, Croce CM. Potential of microRNAs for cancer diagnostics, prognostication and therapy. *Curr Opin Oncol*. 2012;24(6):655–659. doi:10.1097/CCO.0b013e328358522c
16. Lu GJ, Dong YQ, Zhang QM, et al. miRNA-221 promotes proliferation, migration and invasion by targeting TIMP2 in renal cell carcinoma. *Int J Clin Exp Pathol*. 2015;8(5):5224–5229.
17. Ding D, Zhang Y, Wen L, et al. MiR-367 regulates cell proliferation and metastasis by targeting metastasis-associated protein 3 (MTA3) in clear-cell renal cell carcinoma. *Oncotarget*. 2017;8(38):63084–63096. doi:10.18632/oncotarget.18647
18. Wang K, Li Y, Yu D, Zhao J, Ma P. miR-377 functions as a tumor suppressor in human clear cell renal cell carcinoma by targeting ETS1. *Biomed Pharmacother*. 2015;70:64–71. doi:10.1016/j.biopha.2015.01.012
19. Yang FQ, Zhang HM, Chen SJ, Yan Y, Zheng JH. MiR-506 is down-regulated in clear cell renal cell carcinoma and inhibits cell growth and metastasis via targeting FLOT1. *PLoS One*. 2015;10(3):e0120258. doi:10.1371/journal.pone.0120258
20. Wang WJ, Guo CA, Li R, et al. Long non-coding RNA CASC19 is associated with the progression and prognosis of advanced gastric cancer. *Aging*. 2019;11(15):5829–5847. doi:10.18632/aging.102190
21. Wang XD, Lu J, Lin YS, Gao C, Qi F. Functional role of long non-coding RNA CASC19/miR-140-5p/CEMIP axis in colorectal cancer progression in vitro. *World j Gastroenterol*. 2019;25(14):1697–1714. doi:10.3748/wjg.v25.i14.1697
22. Wang JJ, Li XM, He L, Zhong SZ, Peng YX, Ji N. Expression and function of long non-coding RNA CASC19 in colorectal cancer. *Zhongguo Yi Xue Ke Xue Yuan Xue Bao Acta Academiae Medicinae Sinicae*. 2017;39(6):756–761. doi:10.3881/j.issn.1000-503X.2017.06.004
23. Qu CX, Shi XC, Zai LQ, Bi H, Yang Q. LncRNA CASC19 promotes the proliferation, migration and invasion of non-small cell lung carcinoma via regulating miRNA-130b-3p. *Eur Rev Med Pharmacol Sci*. 2019;23(3 Suppl):247–255. doi:10.26355/eurrev_201908_18654
24. Livak KJ, Schmittgen TD. Analysis of relative gene expression data using real-time quantitative PCR and the 2(-Delta Delta C(T)) Method. *Methods*. 2001;25(4):402–408. doi:10.1006/meth.2001.1262
25. Wang L, Cho KB, Li Y, Tao G, Xie Z, Guo B. Long noncoding RNA (lncRNA)-mediated competing endogenous RNA networks provide novel potential biomarkers and therapeutic targets for colorectal cancer. *Int J Mol Sci*. 2019;20:22.
26. Zhai W, Ma J, Zhu R, et al. MiR-532-5p suppresses renal cancer cell proliferation by disrupting the ETS1-mediated positive feedback loop with the KRAS-NAP1L1/P-ERK axis. *Br J Cancer*. 2018;119(5):591–604. doi:10.1038/s41416-018-0196-5

27. Wang G, Zhang ZJ, Jian WG, et al. Novel long noncoding RNA OTUD6B-AS1 indicates poor prognosis and inhibits clear cell renal cell carcinoma proliferation via the Wnt/beta-catenin signaling pathway. *Mol Cancer*. 2019;18(1):15. doi:10.1186/s12943-019-0942-1
28. Dong D, Mu Z, Wei N, et al. Long non-coding RNA ZFAS1 promotes proliferation and metastasis of clear cell renal cell carcinoma via targeting miR-10a/SKA1 pathway. *Biomed Pharmacother*. 2019;111:917–925. doi:10.1016/j.biopha.2018.12.143
29. Zheng Z, Zhao F, Zhu D, et al. Long non-coding RNA LUCAT1 promotes proliferation and invasion in clear cell renal cell carcinoma through AKT/GSK-3beta signaling pathway. *Cell Physiol Biochem*. 2018;48(3):891–904. doi:10.1159/000491957
30. Qu L, Wang ZL, Chen Q, et al. Prognostic value of a long non-coding RNA signature in localized clear cell renal cell carcinoma. *Eur Urol*. 2018;74(6):756–763. doi:10.1016/j.eururo.2018.07.032
31. Zhang X, Wu J, Wu C, et al. The LINC01138 interacts with PRMT5 to promote SREBP1-mediated lipid desaturation and cell growth in clear cell renal cell carcinoma. *Biochem Biophys Res Commun*. 2018;507(1–4):337–342. doi:10.1016/j.bbrc.2018.11.036
32. Abdollahzadeh R, Daraei A, Mansoori Y, Sepahvand M, Amoli MM, Tavakkoly-Bazzaz J. Competing endogenous RNA (ceRNA) cross talk and language in ceRNA regulatory networks: a new look at hallmarks of breast cancer. *J Cell Physiol*. 2019;234(7):10080–10100. doi:10.1002/jcp.27941
33. Dittmer J. The role of the transcription factor Ets1 in carcinoma. *Semin Cancer Biol*. 2015;35:20–38. doi:10.1016/j.semcancer.2015.09.010
34. Furlan A, Vercamer C, Bouali F, et al. Ets-1 controls breast cancer cell balance between invasion and growth. *Int j Cancer*. 2014;135(10):2317–2328. doi:10.1002/ijc.28881
35. Liao H, Pan Y, Pan Y, et al. MicroRNA874 is downregulated in cervical cancer and inhibits cancer progression by directly targeting ETS1. *Oncol Rep*. 2018;40(4):2389–2398. doi:10.3892/or.2018.6624
36. Zheng L, Qi T, Yang D, et al. microRNA-9 suppresses the proliferation, invasion and metastasis of gastric cancer cells through targeting cyclin D1 and Ets1. *PLoS One*. 2013;8(1):e55719. doi:10.1371/journal.pone.0055719
37. Mikami S, Oya M, Mizuno R, Murai M, Mukai M, Okada Y. Expression of Ets-1 in human clear cell renal cell carcinomas: implications for angiogenesis. *Cancer Sci*. 2006;97(9):875–882. doi:10.1111/j.1349-7006.2006.00268.x